Adsorption (2010) 16: 465–472
DOI 10.1007/s10450-010-9248-8

A family of ordered mesoporous carbons derived from mesophase pitch using ordered mesoporous silicas as templates

Liang Cao · Michal Kruk

Received: 4 May 2010 / Accepted: 8 July 2010 / Published online: 31 July 2010

Abstract A variety of ordered mesoporous carbons (OMCs) were synthesized using ordered mesoporous silicas (OMSs) as hard templates and the mesophase pitch (MP) as a carbon precursor. The synthesis included the mixing of OMS with MP, the infiltration of OMS with MP at 450–550 °C and the carbonization of MP in OMS/MP composite followed by the dissolution of the OMS template. OMCs with structures of two-dimensional hexagonal arrays of nanorods and three-dimensional arrays of nanospheres were obtained through the replication of silica templates, including large-pore SBA-15, KIT-6, large-pore FDU-12 and SBA-16. In particular, 2-D hexagonal array of carbon nanorods (CMK-3 carbon) with (100) interplanar spacing of ∼13 nm as well as an array of carbon nanospheres arranged in the face-centered cubic structure with the unit-cell parameter of 33 nm were successfully prepared. The specific surface areas of the resulting carbons were up to 400 m^2/g, and the total pore volumes were up to 0.43 cm^3/g, with the highest values achieved when the MP infiltration temperature was 500 °C. The OMCs exhibited narrow mesopore size distributions. As inferred from XRD, the frameworks of OMCs featured semi-graphitic structures even though moderate carbonization temperature (850 °C) was employed.

L. Cao · M. Kruk
Center for Engineered Polymeric Materials, Department of Chemistry, College of Staten Island, City University of New York, 2800 Victory Boulevard, Staten Island, NY 10314, USA

L. Cao · M. Kruk (✉)
Graduate Center, City University of New York, 365 Fifth Avenue, New York, NY 10016, USA
e-mail: Michal.Kruk@csi.cuny.edu

Keywords Ordered mesoporous carbon · Templated synthesis · Ordered mesoporous silica · Mesophase pitch · High-surface-area solid

1 Introduction

Ordered mesoporous carbons (OMCs) (Ryoo et al. 2001; Lee et al. 2006; Liang et al. 2008) are unique porous carbonaceous materials due to their ordered nanoscale structures, pore sizes in the mesopore range (typically 2–12 nm), high specific surface areas and large pore volumes. OMCs have attracted a lot of attention, mainly due to their potential advanced applications in the areas of heterogeneous catalysis, chromatography, electrochemical double-layer capacitors and gas storage.

The syntheses of OMCs are based on two strategies, namely soft templating (Liang et al. 2004; Tanaka et al. 2005; Zhang et al. 2005) and hard templating (Lee et al. 1999; Ryoo et al. 1999; Jun et al. 2000; Joo et al. 2001; Kleitz et al. 2003; Li et al. 2004; Yang et al. 2004; Vix-Guterl et al. 2003; Li et al. 2005; Li and Dai 2005; Kruk et al. 2005; Li and Jaroniec 2004). The former method utilizes self-assembled amphiphilic molecules (surfactants) or block copolymers as templates to direct carbon precursors to form cross-linked polymeric network with periodically arranged voids, which is followed by removal of the template, and carbonation (or in some cases, even graphitization (Wang et al. 2008)) of the carbon precursor. However, a more frequently used strategy is the hard templating or nano-casting method (Ryoo et al. 2001; Lee et al. 1999; Ryoo et al. 1999; Knox et al. 1986; Knox et al. 1983; Goeltner and Weissenberger 1998; Yang and Zhao 2005), in which solid nanoporous structures are applied as templates to assist carbon precursors to form mesoporous struc-

tures. The strategy usually involves three major steps: (i) introduction of the carbon precursor to the pores of the template, (ii) the carbonation of the carbon precursor in the carbon/template composite and (iii) the removal of the template. The method affords porous carbons that retain the morphology of the template (if the latter has a 3-D pore connectivity) (Ryoo et al. 1999, 2001; Jun et al. 2000), but are inverse replicas. The pioneering work on the use of hard templates in the mesoporous carbon synthesis was done by Knox and co-workers (Knox et al. 1983, 1986) who successfully synthesized mesoporous carbons using porous silicas as templates. The first OMC synthesized via hard templating, which is referred to as CMK-1, was a replica of MCM-48 silica with Ia3d symmetry (Lee et al. 1999; Ryoo et al. 1999). Due to the fact that the pore structure of MCM-48 template consists of two disconnected mesopore channel systems, CMK-1 framework consists of two separate parts that slightly shift with respect to one another as the template is removed, resulting in a lower symmetry (Kaneda et al. 2002). Subsequently, the hard templating strategy has been expanded to successfully produce a large variety of OMCs with diverse structures. For instance, 2-D hexagonally ordered arrays of nanorods (CMK-3) (Jun et al. 2000) and nanotubules (CMK-5) (Joo et al. 2001) templated by SBA-15 silica (Zhao et al. 1998; Ryoo et al. 2000) with cylindrical mesopores, and carbons with cubic Ia3d symmetry templated by KIT-6 silica (Kleitz et al. 2003), were obtained. In addition, ordered arrays of carbon nanospheres with Im3m symmetry (Kim et al. 2005b; Guo et al. 2005; Fan et al. 2003; Fulvio et al. 2008; Li et al. 2009) were obtained using SBA-16 silica (Zhao et al. 1998) as a template, and arrays of carbon nanospheres (Kruk et al. 2005; Fan et al. 2003; Fan et al. 2005) were synthesized using FDU-1 (Yu et al. 2000; Matos et al. 2003), FDU-12 (Fan et al. 2003) and large-pore FDU-12 (Fan et al. 2005) with Fm3m symmetry as templates. Many OMCs retained the structural symmetry of their silica templates because of the connectivity between the mesopores of the template and the mechanical stability of the resulting carbon frameworks.

In addition to the synthesis method used, the selection of the carbon precursor is another important factor affecting the properties of the resulting porous carbon. Among various carbon precursors, the mesophase pitch (MP) (Mochida et al. 2000) is particularly interesting, as its stacked layers of polyaromatic rings in liquid crystalline domains facilitate graphitization and render low microporosity (Qiao et al. 2006). MP retains its anisotropic properties in a certain temperature range above its softening point, while the viscosity decreases with temperature until the mesophase-isotropic transition takes place (Mochida et al. 2000). Although mesophase pitch has been known as a precursor for carbon fibers for several decades, its utility to synthesize mesoporous carbons has been explored during the last decade (Li et al. 2002, 2004; Yang et al. 2004; Li and Dai 2005; Li and Jaroniec 2004; Qiao et al. 2006; Li and Jaroniec 2001; Gierszal et al. 2006, 2008; Adelhelm et al. 2007; Mohanty et al. 2009). Li and Jaroniec reported that by using colloidal silica particles to imprint in the mesophase pitch, one can achieve carbons with controlled mesopore size depending on the diameter of the silica particles (Li and Jaroniec 2001). The resulting mesoporous carbons had uniform spherical mesopores with narrow size distribution, quite high specific surface areas (up to 425 m^2/g) and large pore volumes (up to 1.61 cm^3/g), and their heat treatment at 2400 °C under Ar afforded a graphitized carbon with quite narrow mesopore size distribution (Li et al. 2002). Later, the mesophase pitch has been proven useful in the synthesis of OMCs templated by SBA-15 (Yang et al. 2004; Li and Dai 2005; Li and Jaroniec 2004), MCM-48 (Li et al. 2005; Gierszal and Jaroniec 2005), KIT-6 (Gierszal et al. 2008), and SBA-16 (Gierszal and Jaroniec 2005). Moreover, the surfaces of some of these OMCs were functionalized by aryl or fluoro groups to tailor OMC pore diameter and surface properties (Li et al. 2004; Li and Dai 2005).

Taking advantage of MP as an excellent carbon precursor, and a large variety of available OMS templates, mesoporous carbons in the form of ordered arrays of nanorods and nanospheres were synthesized and described herein. It was found that an optimization of the temperature of the MP infiltration step of the synthesis was essential in increasing the specific surface area and facilitated the synthesis of some OMC structures. In particular, OMCs with 2-D hexagonal structures of nanorods (CMK-3 carbons) with large interplanar spacing ($d_{100} = \sim$13 nm) were synthesized. In addition, carbon inverse replicas of SBA-16 and LP-FDU-12 silicas, that is, body-centered cubic and face-centered cubic carbon nanostructures, were successfully obtained, the latter having very large unit-cell size.

2 Materials and methods

2.1 Materials

The synthesis and structural properties of SBA-15 with nominal (BJH) pore diameter ~16 nm and actual pore diameter 14 nm were described in detail elsewhere (the sample was denoted 15C1d+100C2d #2) (Kruk and Cao 2007). SBA-15 with nominal (BJH) pore diameter ~26 nm and actual pore diameter ~19 nm was synthesized at initial temperature of 14 °C and hydrothermally treated at 130 °C for 2 days, as described elsewhere (Cao et al. 2009) (data shown in Supporting Figure S1). Due to the high hydrothermal treatment temperature and extended time, the mesopores of this material are likely to be connected by large mesoporous gaps in the walls (Cao et al. 2009). The synthesis of KIT-6

silica involved a procedure originally reported by Kim et al. (2005a). with the hydrothermal treatment at 100 °C for one day. The synthesis and characterization of LP-FDU-12 silica was described in detail elsewhere (Kruk and Hui 2008) (the sample was denoted 15C + 100C1d + A130C2d). SBA-16 was synthesized using the synthesis mixture composition reported by Kleitz et al. (2006). with the hydrothermal treatment at 130 °C for 2 days. The mesophase pitch (AR-MP) was provided by Mitsubishi Gas Chemical Company. Ground MP was thoroughly mixed with silica template in ethanol (using sonication) and the mixture was dried in an open container until the solvent evaporated. The mixture was transferred into a ceramic boat and heated in a tube furnace under nitrogen atmosphere. The temperature was set at 460–550 °C and maintained for 8 hours (16 hours for SBA-16 replica) (with 5 °C/min ramp to the final temperature) for infiltration, and 850 °C for 3 hours (5 °C/min ramp) for carbonation. The carbon samples were isolated by dissolving the silica templates in HF solution overnight. The products were extensively washed with deionized water and acetone before drying under vacuum. The mass of MP used was calculated as a mass of the template used multiplied by its specific total pore volume and by the density of the mesophase pitch (1.23 g/cm^3), which corresponds to the mass of MP that would be capable of completely filling the mesopores and micropores of the template.

2.2 Measurement

Small-angle X-ray scattering (SAXS) measurements were performed at Station D1 of CHESS synchrotron facility at Cornell University. The samples were placed in a hole in an aluminum sample holder and secured from both sides using a Kapton tape. Powder X-ray diffraction measurements were performed using a PANalytical X-ray Diffractometer with step size of 0.05 ° and angular range of 10–90 °. Transmission electron microscopy (TEM) images were recorded on a Philips CM 100 microscope operated at 80 kV or on a FEI Tecnai G2 Twin microscope operated at 120 kV. Before the imaging, the samples were dispersed in ethanol through sonication and subsequently deposited on a carbon-coated copper grid. Nitrogen adsorption measurements at −196 °C were carried out using a Micromeritics ASAP 2020 volumetric adsorption analyzer. Samples were degassed under vacuum at 200 °C before adsorption measurements. The specific surface area was determined using the BET method (Sing et al. 1985) applied to the relative pressure range 0.04–0.20. The total pore volume was calculated from the amount adsorbed at a relative pressure of 0.99 (Sing et al. 1985). The pore size distribution was calculated from adsorption branches of isotherms using the Barrett-Joyner-Halenda (BJH) algorithm and the KJS relation between the pore diameter and the capillary condensation pressure (Kruk et al. 1997).

3 Results and discussion

3.1 Preparation of 2-D hexagonal arrays of nanorods

SBA-15 with 2-D hexagonal structure of large cylindrical mesopores (Zhao et al. 1998) is one of the most extensive studied and widely applied OMSs because of its facile synthesis and beneficial structural properties. SBA-15 has been proven as an excellent template to fabricate other ordered mesoporous materials, including carbons (CMK-3 and CMK-5) (Jun et al. 2000; Joo et al. 2001; Yang et al. 2004; Vix-Guterl et al. 2003; Li et al. 2005; Li and Dai 2005; Kruk et al. 2005, 2007; Li and Jaroniec 2004) via the inverse replication process. In spite of extensive activity in this area, the use of large-pore SBA-15 (LP-SBA-15; pore diameter >12 nm) as a template has been nearly unexplored. To the best of our knowledge, only Sun et al. (2007) applied macroporous-mesoporous LP-SBA-15 with d_{100} interplanar spacing of ∼14 nm to synthesize an ordered mesoporous carbon (as seen from TEM) that retained the morphology of the template and exhibited narrow pore size distribution (pore diameter ∼6 nm). However, XRD or SAXS data were not reported, so the crucial information about the periodicity and unit-cell size is not available. Straightforward syntheses of LP-SBA-15 with pore diameters up to ∼26 nm have been reported recently (Kruk and Cao 2007; Cao et al. 2009; Sun et al. 2005), and herein the applicability of these templates for the synthesis of CMK-3 carbons is demonstrated.

The LP-SBA-15 template applied in our study had a large (100) interplanar spacing (14.0 nm), a large pore diameter of 14.3 nm (nominal BJH pore diameter ∼16 nm), high surface area (550 m^2/g) and large pore volume (1.36 cm^3/g) (Kruk and Cao 2007). The process of infiltration with the carbon precursor (MP) is illustrated in Fig. 1. When the temperature was raised above MPs softening temperature (∼285 °C), MP became less viscous and infiltrated the cylindrical nanochannels of LP-SBA-15. The subsequent carbonation process at 850 °C was likely to facilitate intermolecular cross-linking to form semi-graphitic carbon framework (see below). Finally, the silica template was removed by HF etching. The resulting carbon samples showed highly ordered 2-D hexagonal (CMK-3 type) structures, as seen from SAXS patterns (Fig. 2(a)) with diffraction peaks indexed as (100), (110) and (200). The formation of inverse replicas of SBA-15 in the case of carbon and other framework compositions has been explained as a result of the micropore/mesopore connections between the ordered mesopores of SBA-15, as these connecting pores allow for the formation of connections between the nanorods in the structure of the inverse replica (Jun et al. 2000). It is demonstrated herein that the increase in the unit-cell size and a related increase in the pore wall thickness does

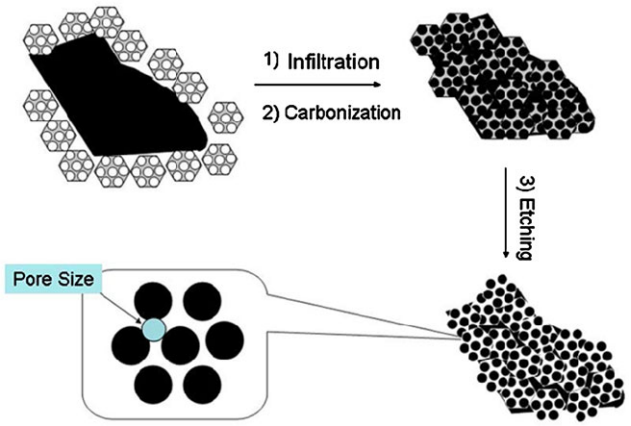

Fig. 1 The scheme of the process for preparing ordered mesoporous carbons using the template (e.g., large-pore SBA-15 silica) and the mesophase pitch carbon precursor. The pore diameter of the 2-D hexagonal arrays of nanorods provides the information about the dimensions of space between three adjacent nanorods

not have an adverse effect on the ability to form highly ordered CMK-3 carbons. There is no obvious difference in (100) interplanar spacings (∼13 nm) for all the CMK-3 samples synthesized with different infiltration temperatures, indicating a good reproducibility of the dimensions of the nanostructure. A low extent of contraction of the unit cell during the carbon formation process (from $d_{100} = 14$ nm for the silica template to 13 nm) can be attributed to a high carbon yield for the pitch carbonization and an excellent thermal stability of the silica template and the produced carbon nanostructure.

The obtained carbon samples were further analyzed by nitrogen adsorption. As shown in Fig. 2(b), the carbon samples prepared at different infiltration temperatures had similar Type IV adsorption-desorption isotherms. The capillary condensation steps occurred in the relative pressure range from 0.45 to 0.65 and the isotherms leveled off at higher relative pressure, indicating uniform pore structures and low

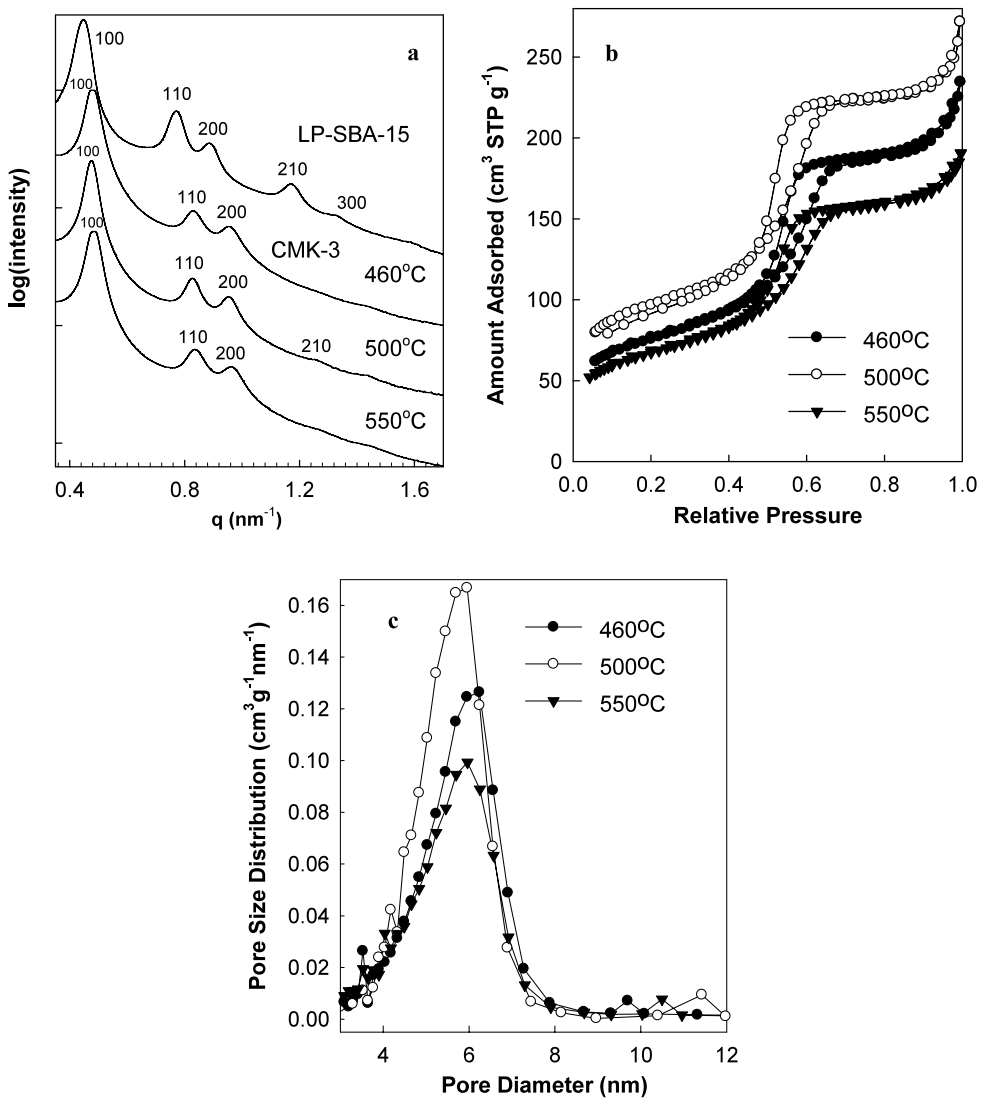

Fig. 2 (**a**) SAXS patterns, (**b**) nitrogen adsorption isotherms and (**c**) pore size distributions of mesoporous carbon samples prepared using the LP-SBA-15 template and different MP infiltration temperatures

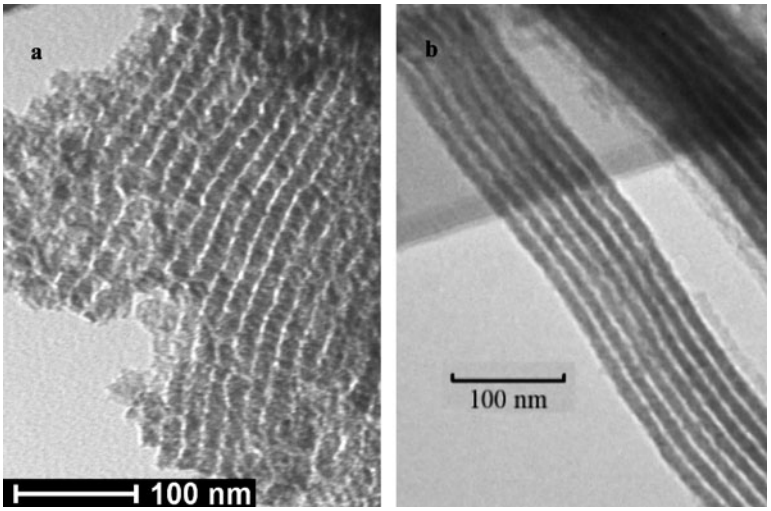

Fig. 3 TEM images of mesoporous carbons prepared using LP-SBA-15 templates of pore diameter (**a**) ∼19 nm, and (**b**) 14 nm. The infiltration temperature was 500 °C

external surface areas. The adsorption isotherms of our carbons were similar to that reported by Sun et al. (2007) for their macroporous-mesoporous carbon prepared using a similar template. However, these researchers did not report X-ray diffraction/scattering data, so overall periodicity of their carbon is not clear.

Interestingly, the BET specific surface area and pore volume of the CMK-3 samples reached the maximum (340 m^2/g and 0.40 cm^3/g, respectively) when the infiltration temperature was 500 °C. It is known that the viscosity of the MP will gradually decrease with the rising temperature so the higher temperature is likely to be beneficial for MP infiltration into LP-SBA-15 nano-channels and thus expected to lead to higher pore volume and specific surface area. However, the phenomenon observed here might be due to the cross-linking of pitch molecules when imprinting temperature is much higher (e.g., 550 °C) than the MP softening temperature, and close to the carbonation temperature (850 °C), and/or to the mesophase–isotropic phase transition (Mochida et al. 2000) taking place at excessively high temperatures. Either possibility would lead to higher viscosity and reduced mobility of MP, which may have negative effect on the BET specific surface area and pore volume. To rule out the possibility of an effect specific to LP-SBA-15 template, another template (KIT-6) with 3-D cubic structure was studied and found to exhibit a similar trend (data not shown).

The BET specific surface area and pore volume of the obtained carbons are much less than those for carbons produced from many other carbon precursors, especially sucrose, as these precursors give rise to carbons with considerable amount of microporosity, leading to very high specific surface area and pore volume (Jun et al. 2000). However, OMCs from mesophase pitch and some other precursors giving rise to semi-graphitic carbon frameworks with low microporosity (Li and Jaroniec 2004; Gierszal et al. 2008) commonly exhibit specific surface areas and pore volumes comparable to the carbons from our optimized synthesis. The pore size distributions (PSDs) in Fig. 2(c) indicated that the pore diameters of the carbon samples were independent of the imprinting temperature. PSDs were relatively narrow and had a maximum around 5.8 nm. This pore size is larger than pore wall thickness of the LP-SBA-15 template (∼2 nm) because the pore diameter shown on PSD reflects primarily the dimensions of the pore space between three adjacent carbon nanorods (see Fig. 1) (Joo et al. 2002). The pore diameter of CMK-3 prepared from MP using large-pore SBA-15 was larger than the pore diameter of CMK-3 templated by regular SBA-15 silica derived from MP (Li and Jaroniec 2004) or petroleum pitch (Vix-Guterl et al. 2003). This is consistent with Equation (3) of Joo et al. (2002), which indicates that the pore diameter of CMK-3 scales with the (100) interplanar spacing.

SBA-15 with even larger pore diameter (19 nm, nominal BJH pore diameter 26 nm) was also used to obtain ordered array of carbon nano-rods. TEM images in Fig. 3(a) revealed that both kinds of the SBA-15 inverse replicas contained arrays of uniform nano-rods, whose diameters were roughly estimated from TEM as ∼12 nm and ∼16 nm for carbons templated by the silicas with pore diameters of 14 nm and 19 nm, respectively. It must be pointed out that most of the carbon nanostructures observed in TEM images were nanorods rather than hollow tubes or broken rods, indicating that the MP infiltration process can introduce high loading of carbon to nearly totally fill the mesopores. This provides an insight as to why the tendency to create secondary porosity was not observed and the contraction of the lattice during the inverse replication process was low. The present results show that LP-SBA-15 is a facile template for the synthesis of CMK-3 carbons, which was mentioned elsewhere without presenting the experimental results (Kruk and Cao 2007), the latter being reported here for the first time.

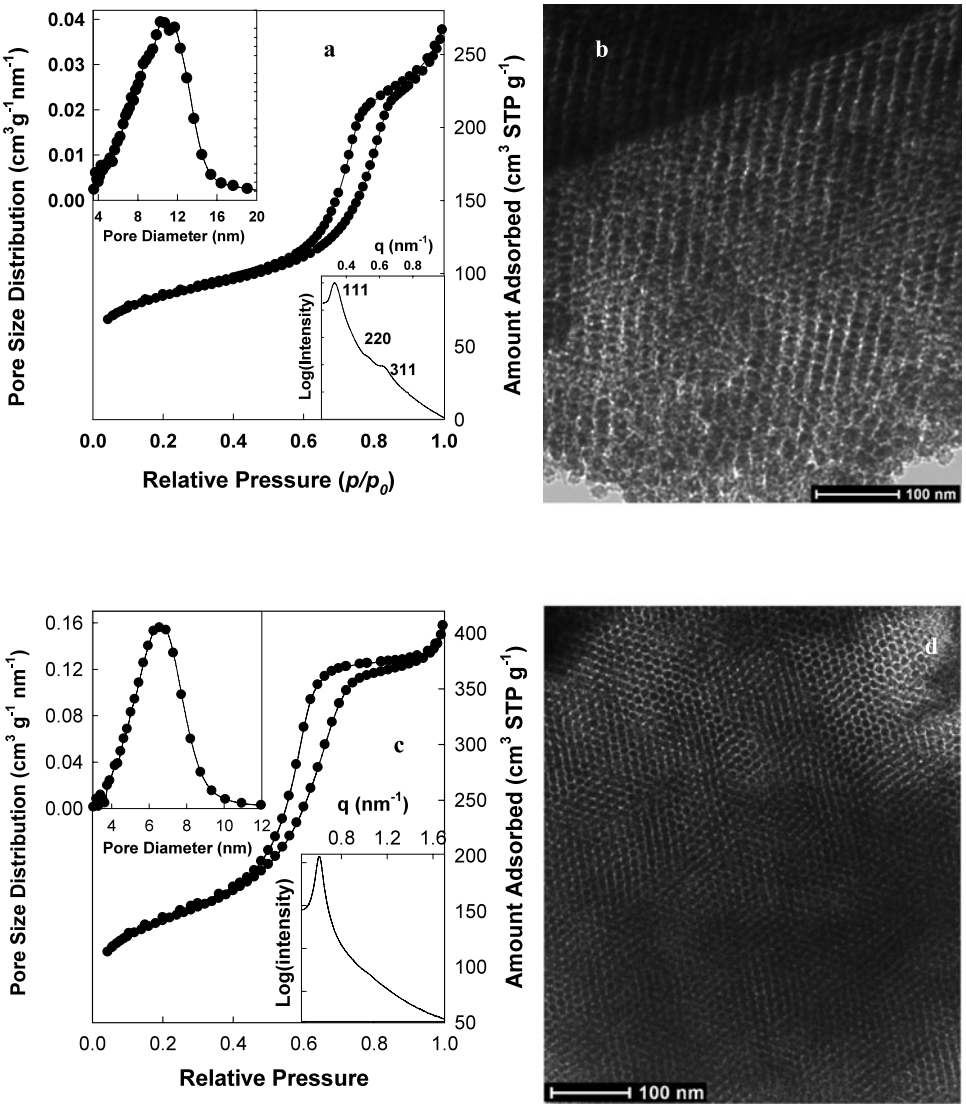

Fig. 4 (**a**) The nitrogen adsorption isotherm with SAXS pattern (*inset*) and pore size distribution (*inset*), and (**b**) TEM image of OMC prepared using the LP-FDU-12 template with infiltration temperature of 500 °C; (**c**) The nitrogen adsorption isotherm with SAXS pattern (*inset*) and pore size distribution (*inset*), and (**d**) TEM image of OMC prepared using the SBA-16 template with infiltration temperature of 500 °C

3.2 Preparation of mesoporous carbons from 3-D OMS templates

The MP infiltration process described above is also capable of producing OMCs using KIT-6 (Kleitz et al. 2003; Kim et al. 2005a) template with 3-D bicontinuous structure and *Ia3d* symmetry (data not shown), as well as SBA-16 (Zhao et al. 1998) with body-centered cubic structure and *Im3m* symmetry, and large-pore FDU-12 (LP-FDU-12) (Fan et al. 2005; Kruk and Hui 2008) with face centered cubic structure and *Fm3m* symmetry.

LP-FDU-12 is OMS with face-centered cubic structure of spherical pores of diameter up to 27 nm, which are connected with one another through passages that can be made large in size (Fan et al. 2005; Kruk and Hui 2008). The successful preparation of OMC using LP-FDU-12 template was indicated by the SAXS pattern that featured peaks and shoulders that can be identified as (111), (220) and (311) reflections of the face-centered cubic structure (Fm3m symmetry) (Fig. 4(a)). Previously, FDU-1, FDU-12 and LP-FDU-12 were used as templates for OMCs (Kruk et al. 2005; Fan et al. 2003; Fan et al. 2005), but the resulting carbons never featured such a well-resolved and indexable XRD or SAXS pattern. The calculated unit cell size was 32.9 nm, which is 9% lower than the unit cell size of 36.3 nm for the silica template. The unit cell size for the considered carbon is particularly large, and exceeds the unit-cell size for LP-FDU-12 carbon described in some detail earlier (Fan et al. 2005). This suggests that the use of LP-FDU-12 templates with large unit-cell size opens an avenue to hard-templated OMCs with unprecedented unit-cell sizes and pore diameters. The BET specific surface area, pore volume and pore diameter of the LP-FDU-12-templated carbon were 297 m^2/g, 0.40 cm^3/g and 10.8 nm (Fig. 4(a)), respectively. The adsorption isotherm was similar to that reported earlier for FDU-1 replica prepared using polyacrylonitrile

as a carbon precursor (Kruk et al. 2005). The TEM image for the LP-FDU-12 inverse replica carbon showed a well-ordered structure composed of nanospheres of size ∼ 20 nm (Fig. 4(b)). OMC was also successfully synthesized using SBA-16 template, which had a body-centered cubic structure and spherical mesopores of diameter ∼11 nm (which is likely to be underestimated by ∼2 nm based on prior studies) (Matos et al. 2003). The resulting OMC obtained via the infiltration with MP at 500 °C for extended period of time had a pore diameter of 6.6 nm, the specific surface area of 500 m^2/g and pore volume of 0.62 cm^3/g (Fig. 4(c)). The adsorption isotherm of our carbon is similar to the isotherms reported earlier for the carbon inverse replicas of SBA-16 (Fan et al. 2003; Fulvio et al. 2009), but in our case, the capillary condensation step was much more pronounced and the isotherm sharply leveled off after the capillary condensation was completed, suggesting the absence of any appreciable secondary mesoporosity. This indicates that the MP affords SBA-16 carbon inverse replicas that are comparable to or even of better quality than those from other carbon sources. The carbon featured a rather narrow single peak on its SAXS pattern. From TEM image (Fig. 4(d)), the estimated diameter of highly ordered nanospheres was ∼11 nm, very close to the pore size of its SBA-16 template.

3.3 Framework properties of carbon samples

To confirm that MP has an advantage of affording semi-graphitic structures (Yang et al. 2004; Gierszal et al. 2008), one of the carbons templated by KIT-6 was examined by XRD. The diffraction pattern featured characteristic (002) reflection at ∼25 ° corresponding to 0.36 nm graphite layer spacing, a less intense peak at ∼44 ° for (100) and/or (101) reflection and a weak (110) reflection at ∼79 ° (Kruk et al. 2007). It is clear that the MP-derived carbon had an appreciable ordering on atomic scale (despite rather low carbonation temperature), but the carbon was still far from a perfectly graphitized structure ($d_{002} = 0.343$ nm). It is known that in the case of templated pitch-based carbons, graphene sheets have preferred perpendicular orientation with respect to the template's mesopore surface (Yang et al. 2004).

4 Conclusions

The results presented here demonstrated that the MP infiltration at 500 °C provided a simple way to synthesize high-quality ordered mesoporous carbons. The method is effective for synthesis of carbons with desired pore geometries, such as 2-D hexagonal arrays of nanorods, or 3-D cubic structures templated by KIT-6, LP-FDU-12 and SBA-16 silicas. The resulting carbons show quite high specific surface areas (up to 500 m^2/g) and moderate pore volumes (up to 0.62 cm^3/g). It is interesting that there was an optimal infiltration temperature (500 °C) under which the resulting carbon sample has the highest surface area and pore volume, which appears to be independent of the type of the template. XRD showed that the obtained mesoporous carbons have semi-graphitic frameworks.

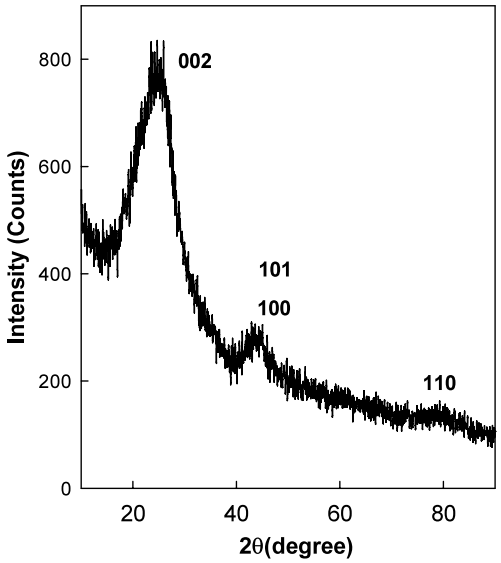

Fig. 5 XRD pattern of KIT-6-templated carbon (infiltration temperature of 500 °C)

Acknowledgement M.K. acknowledges partial support from the Dean of Science and Engineering, CSI/CUNY and from the Center for Engineered Polymeric Materials funded by the New York State Office of Science, Technology and Academic Research (NYSTAR). SAXS measurements were performed at the Cornell High Energy Synchrotron Source (CHESS, Cornell University), which is supported by the National Science Foundation under award DMR-0225180. Dr. Detlef M. Smilgies (CHESS, Cornell University) is gratefully acknowledged for assistance in the SAXS measurements. Mr. Manik Mandal (CSI) is acknowledged for help with TEM imaging, Mr. Chin Ming Hui (CSI) is acknowledged for providing LP-FDU-12 and SBA-16 templates, and Mr. Yu Zhao (City College, CUNY) is acknowledged for help with XRD analysis. Mitsubishi Gas Chemical Company is gratefully acknowledged for providing AR-MP mesophase pitch.

References

Adelhelm, P., Hu, Y.-S., Chuenchom, L., Antonietti, M., Smarsly, B.M., Maier, J.: Adv. Mater. **19**, 4012–4017 (2007)
Cao, L., Man, T., Kruk, M.: Chem. Mater. **21**, 1144–1153 (2009)
Fan, J., Yu, C., Gao, F., Lei, J., Tian, B., Wang, L., Luo, Q., Tu, B., Zhou, W., Zhao, D.: Angew. Chem. Int. Ed. **42**, 3146–3150 (2003)
Fan, J., Yu, C., Lei, J., Zhang, Q., Li, T., Tu, B., Zhou, W., Zhao, D.: J. Am. Chem. Soc. **127**, 10794–10795 (2005)
Fulvio, P.F., Jaroniec, M., Liang, C., Dai, S.: J. Phys. Chem. C **112**, 13126–13133 (2008)
Fulvio, P.F., Vinu, A., Jaroniec, M.: J. Phys. Chem. C **113**, 13565–13573 (2009)
Gierszal, K.P., Jaroniec, M.: Stud. Surf. Sci. Catal. **156**, 581–588 (2005)

Gierszal, K.P., Yoon, S.B., Yu, J.-S., Jaroniec, M.: J. Mater. Chem. **16**, 2819–2823 (2006)
Gierszal, K.P., Jaroniec, M., Kim, T.-W., Kim, J., Ryoo, R.: New J. Chem. **32**, 981–993 (2008)
Goeltner, C.G., Weissenberger, M.C.: Acta Polym. **49**, 704–709 (1998)
Guo, W., Su, F., Zhao, X.S.: Carbon **43**, 2423–2426 (2005)
Joo, S.H., Choi, S.J., Oh, I., Kwak, J., Liu, Z., Terasaki, O., Ryoo, R.: Nature **412**, 169–172 (2001)
Joo, S.H., Ryoo, R., Kruk, M., Jaroniec, M.: J. Phys. Chem. B **106**, 4640–4646 (2002)
Jun, S., Joo, S.H., Ryoo, R., Kruk, M., Jaroniec, M., Liu, Z., Ohsuna, T., Terasaki, O.: J. Am. Chem. Soc. **122**, 10712–10713 (2000)
Kaneda, M., Tsubakiyama, T., Carlsson, A., Sakamoto, Y., Ohsuna, T., Terasaki, O., Joo, S.H., Ryoo, R.: J. Phys. Chem. B **106**, 1256–1266 (2002)
Kim, T.-W., Kleitz, F., Paul, B., Ryoo, R.: J. Am. Chem. Soc. **127**, 7601–7610 (2005a)
Kim, T.-W., Ryoo, R., Gierszal, K.P., Jaroniec, M., Solovyov, L.A., Sakamoto, Y., Terasaki, O.: J. Mater. Chem. **15**, 1560–1571 (2005b)
Kleitz, F., Choi, S.H., Ryoo, R.: Chem. Commun. 2136–2137 (2003)
Kleitz, F., Kim, T.-W., Ryoo, R.: Langmuir **22**, 440–445 (2006)
Knox, J.H., Unger, K.K., Mueller, H.: J. Liq. Chromatogr. **6**, 1–36 (1983)
Knox, J.H., Kaur, B., Millward, G.R.: J. Chromatogr. **352**, 3–25 (1986)
Kruk, M., Cao, L.: Langmuir **23**, 7247–7254 (2007)
Kruk, M., Hui, C.M.: Microporous Mesoporous Mater. **114**, 64–73 (2008)
Kruk, M., Jaroniec, M., Sayari, A.: Langmuir **13**, 6267–6273 (1997)
Kruk, M., Dufour, B., Celer, E.B., Kowalewski, T., Jaroniec, M., Matyjaszewski, K.: J. Phys. Chem. B **109**, 9216–9225 (2005)
Kruk, M., Kohlhaas, K.M., Dufour, B., Celer, E.B., Jaroniec, M., Matyjaszewski, K., Ruoff, R.S., Kowalewski, T.: Microporous Mesoporous Mater. **102**, 178–187 (2007)
Lee, J., Yoon, S., Hyeon, T., Oh, S.M., Kim, K.B.: Chem. Commun. 2177–2178 (1999)
Lee, J., Kim, J., Hyeon, T.: Adv. Mater. **18**, 2073–2094 (2006)
Li, Z., Dai, S.: Chem. Mater. **17**, 1717–1721 (2005)
Li, Z., Jaroniec, M.: J. Am. Chem. Soc. **123**, 9208–9209 (2001)
Li, Z., Jaroniec, M.: J. Phys. Chem. B **108**, 824–826 (2004)
Li, Z., Jaroniec, M., Lee, Y.-J., Radovic, L.R.: Chem. Commun., 1346–1347 (2002)
Li, Z., Del Cul, G.D., Yan, W., Liang, C., Dai, S.: J. Am. Chem. Soc. **126**, 12782–12783 (2004)
Li, Z., Yan, W., Dai, S.: Langmuir **21**, 11999–12006 (2005)
Li, W.-C., Nong, G.-Z., Lu, A.-H., Hu, H.-Q.: J. Porous Mater. (2009, in press). doi:10.1007/s10934-009-9352-x
Liang, C., Hong, K., Guiochon, G.A., Mays, J.W., Dai, S.: Angew. Chem. Int. Ed. **43**, 5785–5789 (2004)
Liang, C., Li, Z., Dai, S.: Angew. Chem. Int. Ed. **47**, 3696–3717 (2008)
Matos, J.R., Kruk, M., Mercuri, L.P., Jaroniec, M., Zhao, L., Kamiyama, T., Terasaki, O., Pinnavaia, T.J., Liu, Y.: J. Am. Chem. Soc. **125**, 821–829 (2003)
Mochida, I., Korai, Y., Ku, C.-H., Watanabe, F., Sakai, Y.: Carbon **38**, 305–328 (2000)
Mohanty, P., Fei, Y., Landskron, K.: J. Am. Chem. Soc. **131**, 9638–9639 (2009)
Qiao, W.M., Song, Y., Hong, S.H., Lim, S.Y., Yoon, S.H., Korai, Y., Mochida, I.: Langmuir **22**, 3791–3797 (2006)
Ryoo, R., Joo, S.H., Jun, S.: J. Phys. Chem. B **103**, 7743–7746 (1999)
Ryoo, R., Ko, C.H., Kruk, M., Antochshuk, V., Jaroniec, M.: J. Phys. Chem. B **104**, 11465–11471 (2000)
Ryoo, R., Joo, S.H., Kruk, M., Jaroniec, M.: Adv. Mater. **13**, 677–681 (2001)
Sing, K.S.W., Everett, D.H., Haul, R.A.W., Moscou, L., Pierotti, R.A., Rouquerol, J., Siemieniewska, T.: Pure Appl. Chem. **57**, 603–619 (1985)
Sun, J., Zhang, H., Ma, D., Chen, Y., Bao, X., Klein-Hoffmann, A., Pfaender, N., Su, D.S.: Chem. Commun. 5343–5345 (2005)
Sun, J., Ma, D., Zhang, H., Bao, X., Weinberg, G., Su, D.: Microporous Mesoporous Mater. **100**, 356–360 (2007)
Tanaka, S., Nishiyama, N., Egashira, Y., Ueyama, K.: Chem. Commun. 2125–2127 (2005)
Vix-Guterl, C., Saadallah, S., Vidal, L., Reda, M., Parmentier, J., Patarin, J.: J. Mater. Chem. **13**, 2535–2539 (2003)
Wang, X., Liang, C., Dai, S.: Langmuir **24**, 7500–7505 (2008)
Yang, H., Zhao, D.: J. Mater. Chem. **15**, 1217–1231 (2005)
Yang, H., Yan, Liu, Y., Zhang, F., Zhang, R., YanMeng, Y., Li, M., Xie, S., Tu, B., Zhao, D.: J. Phys. Chem. B **108**, 17320–17328 (2004)
Yu, C., Yu, Y., Zhao, D.: Chem. Commun., 575–576 (2000)
Zhang, F., Meng, Y., Gu, D., Yan, Yu, C., Tu, B., Zhao, D.: J. Am. Chem. Soc. **127**, 13508–13509 (2005)
Zhao, D., Huo, Q., Feng, J., Chmelka, B.F., Stucky, G.D.: J. Am. Chem. Soc. **120**, 6024–6036 (1998)